J Appl Electrochem (2014) 44:831–840
DOI 10.1007/s10800-014-0691-1

RESEARCH ARTICLE

Poly(acridine orange)-modified glassy carbon electrodes: electrosynthesis, characterisation and sensor application with uric acid

Dilek Kul · Burcu Doğan-Topal · Sibel A. Özkan · Bengi Uslu

Received: 24 January 2014 / Accepted: 16 April 2014 / Published online: 14 May 2014

Abstract Poly(acridine orange) was electropolymerised on glassy carbon electrodes by potential cycling in phosphate buffer solution at pH 5.5, 6.0, 7.0 and 8.0. Electrochemical behaviour of the modified electrodes was studied by cyclic voltammetry in phosphate buffer solution at various pHs and found that the best polymer film formation was obtained at pH 5.5. Quantitative determination of uric acid was achieved by cyclic voltammetry, differential pulse voltammetry (DPV) and fixed-potential amperometry in phosphate buffer solution at pH 5.5. Anodic peak currents were linearly proportional to concentration of uric acid in the range 1–75 μM for cyclic voltammetry, 0.4–75 μM for DPV and 0.04–5.3 μM for amperometry. Detection limits were 3.7×10^{-1}, 9.7×10^{-2} and 9.5×10^{-3} μM for cyclic voltammetry, DPV and amperometry, respectively. The modified electrodes exhibited good sensitivity, wide linear range and good stability. There is no interference from substances commonly present in natural samples.

Keywords Acridine orange · Electropolymerisation · Cyclic voltammetry · Differential pulse voltammetry · Amperometry · Uric acid determination

D. Kul
Department of Analytical Chemistry, Faculty of Pharmacy, Karadeniz Technical University, 61080 Trabzon, Turkey

B. Doğan-Topal · S. A. Özkan · B. Uslu (✉)
Department of Analytical Chemistry, Faculty of Pharmacy, Ankara University, 06100 Tandogan, Ankara, Turkey
e-mail: buslu@pharmacy.ankara.edu.tr

1 Introduction

Conductive polymers prepared by electropolymerisation have recently become attractive due to their wide range of applications such as electrochromic display devices, capacitors, protective coatings for corrosion control, electromagnetic shielding devices and chemical sensors [1, 2]. The conductive polymers synthesised by electropolymerisation of azines and phenazines can serve as redox mediators [3–8]. Active sites of these dyes facilitate the electrochemical deposition of electroactive species. In addition, some functional groups of the polymers such as –NH and –COOH allow selective molecular interactions between the polymer film and the target molecule. The polymer-modified electrodes have been widely used in electrochemical sensors and biosensors for the investigation of the characteristics of some molecules such as L-cysteine and L-tyrosine [3], dopamine [4, 5], caffeine [6], nitric oxide [7] and hydrogen peroxide [8].

Acridine orange (AO), *N*,*N*,*N*′,*N*′-tetramethylacridine-3,6-diamine, is a nitrogen-containing aromatic dye (Scheme 1) generally used as a nucleic acid selective fluorescent cationic dye for cell cycle determination [9]. It has also been used as a probe for measuring pH gradients in membrane vesicles [10]. Aggregation feature of AO has a great importance as a molecular probe for intercalation in DNA [11, 12]. Owing to the structure and molecular recognition capability of AO, it can be polymerised electrochemically on the surface of solid electrodes as a redox mediator for the determination of electroactive molecules such as rutin [13], dobutamine [14] and uric acid (UA) [15].

UA, 2,4,6-trihydroxypurine, is a product of the metabolic breakdown of purine nucleotides. Normal level of UA in human blood plasma is typically between 200 and 430 μM for men and 140 and 360 μM for women.

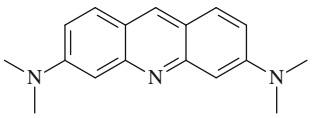

Scheme 1 Structure of acridine orange

Abnormal UA levels in the human body indicate many diseases such as Lesch–Nyhan syndrome, cardiovascular disease, type 2 diabetes, metabolic syndrome, UA stone formation, multiple sclerosis and low zinc level [16]. Hence, fast and reliable determination of UA in biological fluids is significant for diagnosis and treatment of the diseases. Many methods such as liquid chromatography and isotopic dilution mass spectrometry [17], chemiluminescence [18] and uricase immobilization [19] have been described for the detection of UA. However, these methods are relatively expensive, complex and time-consuming. Electroanalytical techniques have often been used for the determination of UA due to their advantages such as high sensitivity, selectivity, low cost, simplicity and short analysis time [20, 21].

The aim of this work is to investigate the electropolymerisation of AO on the surface of glassy carbon (GC) electrodes forming poly(acridine orange), poly(AO), films under the optimised polymerisation conditions. Electrochemical characterisation of poly(AO)-modified electrodes was carried out by cyclic voltammetry (CV) in various electrolyte solutions. The prepared electrodes were used for the electrochemical determination of UA by CV, differential pulse voltammetry (DPV) and fixed-potential amperometry. Interference study was also carried out using different compounds commonly present in natural samples.

2 Experimental

2.1 Materials

AO as a hemi-zinc chloride salt ($C_{17}H_{20}ClN_3 \cdot HCl \cdot 1/2ZnCl_2$) and UA were purchased from Fluka (U.K.) and Aldrich (Germany), respectively, and used without further purification. Phosphate buffer solutions (PBS, 25 mM) at pH 5.5, 6.0, 7.0 and 8.0 were prepared from sodium dihydrogenphosphate (Aldrich, Germany) and di-sodium hydrogenphosphate (Aldrich, Germany), and then the pH was adjusted with 5 M NaOH (Aldrich, Czech Republic) solution. The electrolytes used for the polymerisation and characterisation studies were 50 mM KCl (Riedel-de Haën, Germany) and 50 mM KNO_3 (Merck, Germany).

Ascorbic acid and dopamine were from Acros (Hungary) and Aldrich (U.S.A.), respectively, and used without purification.

Millipore Milli-Q nanopure water (resistivity $\geq$ 18 MΩ cm) and analytical grade reagents were used for the preparation of all solutions. All experiments were performed at room temperature, 25 ± 1 °C.

2.2 Instrumentation

A three-electrode electrochemical cell was used for the experiments. It contained a GC working electrode (BAS, Φ: 3 mm diameter), a platinum wire as counter electrode and a Ag/AgCl electrode as reference.

All measurements by CV, DPV and fixed-potential amperometry were performed using a computer-controlled Autolab Type II potentiostat/galvanostat with GPES 4.9 software (Metrohm-Autolab, The Netherlands).

The pH measurements were carried out using a model 538-pH meter (WTW, Weilheim, Germany) with an accuracy of ±0.05 pH at room temperature.

2.3 Preparation of poly(AO)-modified electrodes

A GC working electrode was polished using Al_2O_3 slurry on a polishing pad and then rinsed with nanopure water. Before use, electrochemical pre-treatment of the electrode was done by cycling in the potential range between −0.6 and +1.2 V at a scan rate of 100 mV s^{-1} in 25 mM PBS at pH 5.5. Thus, the background currents decreased and the potential window increased.

The poly(AO) films were obtained by electropolymerisation by cycling in the potential range between −0.3 and +1.2 V versus Ag/AgCl at a scan rate of 100 mV s^{-1} for 20 cycles in 25 mM PBS at pH 5.5, 6.0, 7.0 and 8.0. Various concentrations of AO monomer in 25 mM PBS, 0.1, 0.2, 0.5 and 1.0 mM, were studied for the electropolymerisation.

2.4 Voltammetric studies

UA was used for the sensor application of poly(AO)-modified GC electrodes. Validation of the studied method for UA was carried out with ruggedness, precision and accuracy by assaying five replicate samples on the same day. Relative standard deviations (RSD %) were also calculated to check the ruggedness and precision of the methods [22, 23].

All working solutions were freshly prepared before the experiments and protected from the light. Measurements were done at room temperature. The calibration equations were constructed using DPV and fixed-potential amperometry by plotting the peak current against the concentration of UA.

3 Results and discussion

3.1 Electropolymerisation of AO

AO was polymerised electrochemically on the surface of GC electrodes by potential cycling for 20 cycles in the potential range between −0.3 and 1.2 V versus Ag/AgCl in 25 mM PBS at pH 5.5, 6.0, 7.0 and 8.0. Various AO monomer concentrations, 0.1, 0.2, 0.5 and 1.0 mM, were used to find the best polymerisation. Cyclic voltammograms of 0.5 mM AO recorded during the potential cycling in different buffers are shown in Fig. 1.

The oxidation of AO monomer undergoes with one electron process. After the unpaired electron is delocalized in the radical cation, the attacking site of AO molecules is probably either the $-N(CH_3)_2$ group or the neighbouring ortho carbon atom in the aromatic ring. Thus, dimerisation forms with a C–N bond and, then radical cations of the dimmers can react with the other monomers. This route leads to form poly(AO) film on the surface of GC electrodes [24].

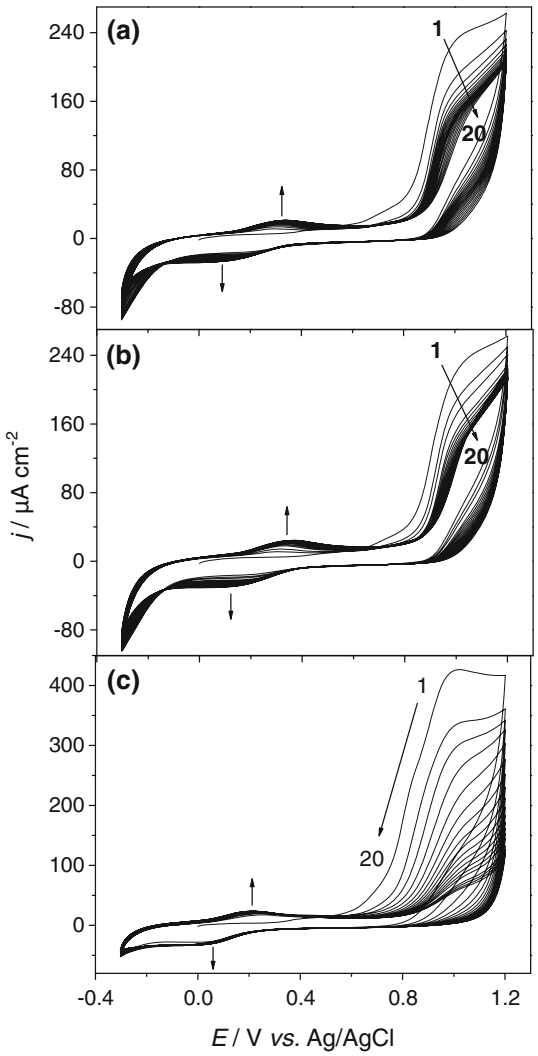

Fig. 1 Cyclic voltammograms of 0.5 mM AO in 25 mM PBS at **a** pH 5.5 **b** pH 6.0 and **c** pH 7.0. Scan rate: 100 mV s^{-1}

According to Fig. 1, monomer radical formation gave an irreversible oxidation peak at +0.98 V and the peak current decreased with the continuing cycling. Cyclic voltammograms also showed the oxidation/reduction peaks of the monomer and polymer. A redox couple at around +0.2 V corresponds to oxidation/reduction of the polymer. With the continuing cycling, the oxidation peak of the polymer at +0.32 V increased in height and its peak potential shifted in the positive direction: the reduction peak of the polymer at +0.13 V also increased and shifted to more negative potentials, showing the formation of the polymer film. The shift of the polymer redox peaks indicates the changes in polymer structure due to the formation of dimmers and trimmers, then oligomerisation and finally polymer growth. A very small anodic wave at around +0.72 V corresponds to monomer, but no related cathodic peak could be observed in the reverse scan. The oxidation peak current of the monomer decreased with the number of cycles and its peak potential shifted in the positive direction. Since the peak potentials of AO monomer and poly(AO) film were close and the peak current of poly(AO) was much higher than that of AO, the peak of poly(AO) enclosed the peak of AO with the growth of polymer. For this reason, the polymer peaks could be observed much better in CVs (Fig. 1). After the polymerisation, the surface of GC electrode had a yellow-brown colour due to poly(AO) film.

The electropolymerisation of AO was carried out in 25 mM PBS at various pH values to obtain the best polymerisation media. The fastest and well-defined poly(AO) film formation was obtained in 25 mM PBS at pH 5.5 (Fig. 1a). The highest peak currents of poly(AO) redox peaks were also obtained in this media. By the 20th cycle, the peak of AO monomer at +0.72 V completely disappeared and the height of poly(AO) peaks decreased, meaning formation of polymer stopped by the 20th cycle (Fig. 1a). For the other AO polymerisations in 25 mM PBS containing 0.5 mM AO, the polymer redox peaks at ~+0.2 V decreased after the following numbers of cycle: the 7th cycle at pH 6.0 (Fig. 1b) and the 3rd cycles at both pH 7.0 (Fig. 1c) and pH 8.0. The reason of early decrease of polymerisation might be low solubility of AO in neutral and basic solutions due to benzene ring and amino group, which is not protonated at these pHs [25, 26].

The influence of chloride (Cl^-) and nitrate (NO_3^-) ions on the electropolymerisation of AO was also investigated, since the electropolymerisation of some other phenazines such as safranine T [27], neutral red [28] and methylene green [28] was faster in buffer solutions including potassium

chloride (KCl) or potassium nitrate (KNO_3). For this purpose, the electropolymerisation of AO was carried out in 50 mM KCl or KNO_3 solutions and 25 mM PBS including 50 mM KCl or KNO_3. However, the polymer growth in the presence of Cl^- and NO_3^- ions was similar to that in 25 mM PBS without these ions.

The polymerisation conditions were optimised in 25 mM PBS in the pH ranges from 5.5 to 8.0 containing various AO monomer concentrations in the range 0.1–1.0 mM. For the polymerisation in 25 mM PBS at pH 5.5, the polymer redox peaks at $\sim+0.2$ V and the radical formation peak at $\sim+0.9$ V increased with increasing AO concentration (Fig. 2). However, the fastest and well-defined polymer film formation was obtained with 0.5 mM AO. Long-chain polymers might not be obtained with higher AO concentrations and short-chain polymers are less adherent to GC electrode. For this reason, 0.5 mM of AO concentration was used for further investigations.

The coverage of poly(AO) film on the surface of GC electrode was calculated using Eq. (1). The calculations of the charge corresponding to the polymer oxidation (Q) and the surface concentration (Γ) of poly(AO) were done from CVs at a scan rate of 100 mV s^{-1}. It was assumed that one electron was involved per monomer in the electropolymerisation process of AO [29].

$$\Gamma = Q / nFA \quad (1)$$

where n is the number of electrons, A is the electrode surface area (cm^2), and F is the Faraday constant. The results of the charge corresponding to polymer oxidation and the surface concentration are listed in Table 1. These values increased with increasing pH of 25 mM PBS until pH 6.0. After pH 6.0, the charge and the surface concentration decreased. It showed that the thickest poly (AO) film was obtained in 25 mM PBS at pH 6.0, named as $poly(AO)_2$ in Table 1.

3.2 Electrochemical characterisation of poly(AO)

Electrochemical characterisation of poly(AO)-modified electrodes presented in Table 1 was achieved by CVs at the scan rates in the range 5–200 mV s^{-1} in 50 mM KCl, 50 mM KNO_3 and 25 mM PBS at pH 5.5, 6.0, 7.0 and 8.0. More acidic buffers than pH 5.5 and more alkaline buffers than pH 8.0 were not used to protect the stability of poly(AO) films. The polymer film named as $poly(AO)_1$ (Fig. 3a) gave the best peak shapes and the highest slopes of the peak current density versus the scan rate for both anodic and cathodic ways in 25 mM PBS at pH 5.5 comparing to the other poly(AO) films (Table 2). For this reason, $poly(AO)_1$-modified GC electrode was selected for the study of UA determination.

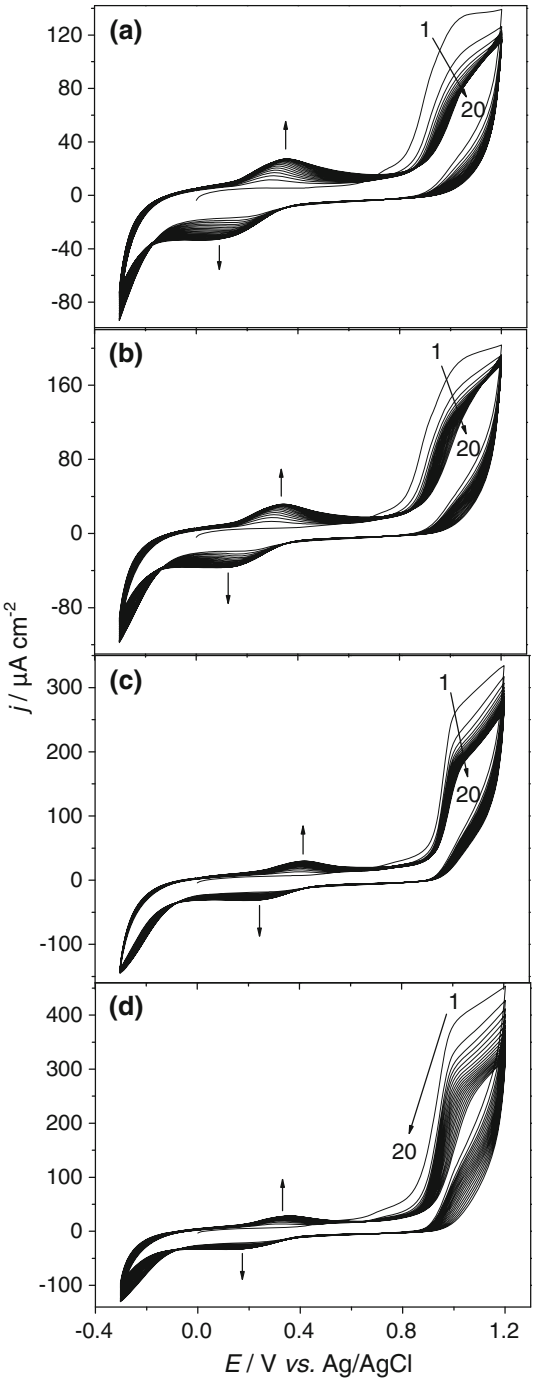

Fig. 2 Cyclic voltammograms of **a** 0.1 mM, **b** 0.2 mM, **c** 0.5 mM and **d** 1.0 mM AO in 25 mM PBS at pH 5.5. Scan rate: 100 mV s^{-1}

In Fig. 3, the scan rate studies were shown for $poly(AO)_1$-, $poly(AO)_2$-, $poly(AO)_3$- and $poly(AO)_4$-modified GC electrodes at various scan rates in the range 5–200 mV s^{-1} in 25 mM PBS at pH 5.5. One redox peak was observed in the CVs, ascribing to the redox reaction of poly(AO). As the scan rate increased, the oxidation and reduction peak currents increased and the peak potentials shifted to more positive potentials for the oxidation peaks and to more negative

Table 1 Charge corresponding to polymer oxidation (Q) and the surface concentration (Γ) of poly(AO) obtained from polymerisation CVs

Polymer	Buffer used for polymerisation	Q (μC cm^{-2})	Γ (nmol cm^{-2})
Poly(AO)$_1$	25 mM PBS at pH 5.5	16.0	44.0
Poly(AO)$_2$	25 mM PBS at pH 6.0	20.4	56.1
poly(AO)$_3$	25 mM PBS at pH 7.0	17.8	49.1
poly(AO)$_4$	25 mM PBS at pH 8.0	16.1	44.4

AO concentration: 0.5 mM

Scan rate: 100 mV s^{-1}

potentials for the reduction peaks. The plots of the peak current densities (j) versus the scan rate (v) were linear, showing an adsorbed species-controlled electrode process (Table 2). In the meantime, the slope of the oxidation process was higher than the slope of the reduction process. It means that expulsion of the positive counter ion is faster than its diffusion into the polymer film [25, 30].

Separation of the oxidation and reduction peaks was also investigated to evaluate the reversibility of the process. According to Fig. 3a, the peak separation of poly(AO)$_1$ film was 206 mV in 25 mM PBS at pH 5.5 at a scan rate of 100 mV s^{-1}, showing similar results with the other poly(AO) films. The ratio of the oxidation and reduction peak currents, I_{pa}/I_{pc}, at 100 mV s^{-1} was 1.80, meaning a quasi-reversible redox process.

The plots of the peak potentials (E_p) versus pH were linear with similar results for all poly(AO)-modified GC electrodes. The slopes were −64 and −54 mV pH^{-1} for the oxidation and reduction processes, respectively, close to the theoretical value of −59 mV pH^{-1} for a process involving equal numbers of protons and electrons [30]. Thus, the number of electrons and protons assuring the AO polymerisation is one according to the literature [24].

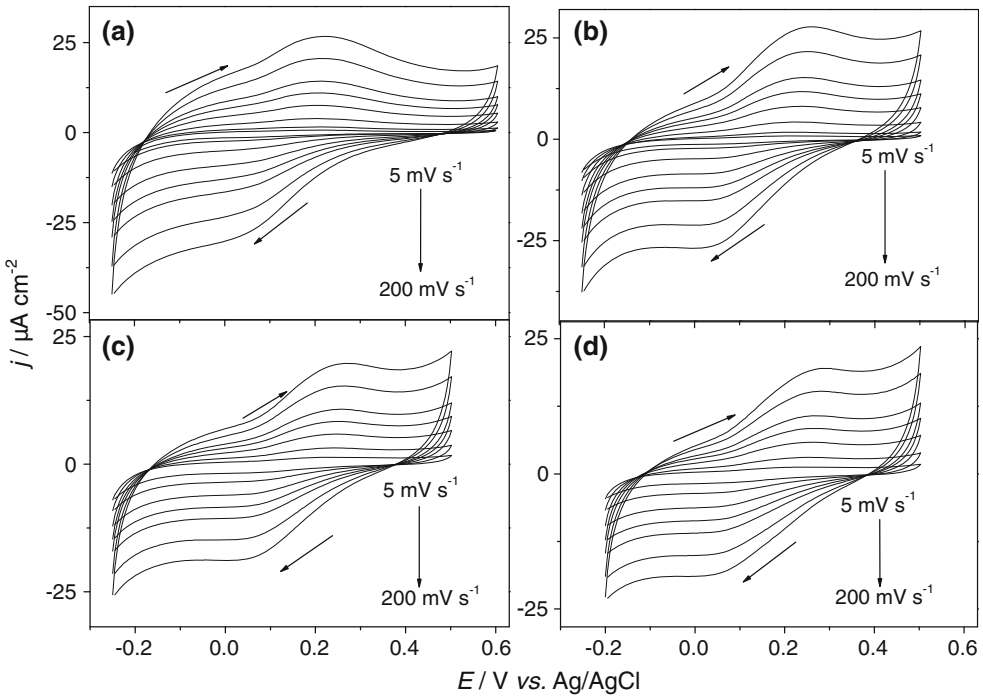

Fig. 3 Cyclic voltammograms of **a** poly(AO)$_1$, **b** poly(AO)$_2$, **c** poly(AO)$_3$ and **d** poly(AO)$_4$ recorded in 25 mM PBS at pH 5.5 at scan rates of 5, 25, 50, 75, 100, 150 and 200 mV s^{-1}

Table 2 Results of the plots of peak current density (j) versus scan rate (v) for poly(AO) films, calculated from the cyclic voltammograms in 25 mM PBS at pH 5.5

Polymer	Oxidation process			Reduction process		
	Slope (μA s cm^{-2} V^{-1})	Intercept (μA cm^{-2})	Correlation coefficient (r)	Slope (μA s cm^{-2} V^{-1})	Intercept (μA cm^{-2})	Correlation coefficient (r)
Poly(AO)$_1$	48.98	0.34	0.997	−35.84	0.12	0.999
Poly(AO)$_2$	41.43	0.30	0.995	−34.73	−0.03	0.999
Poly(AO)$_3$	26.83	0.25	0.995	−29.47	−0.07	0.997
Poly(AO)$_4$	26.80	0.23	0.990	−25.39	−0.11	0.996

Midpoint potentials were also calculated from the average of the anodic and cathodic peak potentials, $E_m = (E_{pa} + E_{pc})/2$ [28], and found as 135 ± 7 mV for poly(AO)$_1$, 150 ± 7 mV for poly(AO)$_2$, 164 ± 4 mV for poly(AO)$_3$ and 173 ± 6 mV for poly(AO)$_4$ versus Ag/AgCl at a scan rate of 100 mV s^{-1} in 25 mM PBS at pH 5.5. Small differences in the midpoint potentials showed the differences in the polymer structures and morphology, since they were polymerised in different buffer solutions.

3.3 Electroanalytical investigation of UA at poly(AO)-modified electrodes

3.3.1 Effect of pH

The dependence of pH on the peak potentials and currents of UA was investigated at poly(AO)$_1$-modified GC electrode in 25 mM PBS at pH 5.5, 6.0, 7.0 and 8.0 containing 80 mM UA using CV and DPV. Since CV and DPV responses were similar, only DP voltammograms are shown in Fig. 4. The peak potentials of UA shifted in the negative direction and the peak currents decreased with increasing pH. Since the highest peak current and the best peak shape were obtained in 25 mM PBS at pH 5.5, this buffer was selected for the determination study of UA. Anodic peak potentials of UA showed a linear dependence on pH with a negative slope of −26.3 mV pH^{-1} and a correlation coefficient of 0.995 by DPV.

3.3.2 Effect of scan rate

The effect of the scan rate on the peak current of UA was investigated in 25 mM PBS at pH 5.5 containing 80 mM UA using CV. The scan rates were in the range 5–200 mV s^{-1}. The oxidation peak current density (j) of UA increased linearly with the square root of the scan rate ($v^{1/2}$) between 5 and 100 mV s^{-1}, showing a diffusion-controlled process in this range (Eq. 2). A loss of linearity of the plot was observed above 100 mV s^{-1}, indicative of the adsorbed species on poly(AO) film-modified GC electrodes at higher scan rates than 100 mV s^{-1}.

$$j\ (\mu A\ cm^{-2}) = 1.109v^{1/2} + 2.92 \quad (r = 0.991) \tag{2}$$

A relationship between the peak potential (E_p) and the scan rate (v) could be expressed by the following Eq. (3):

$$E_p(V) = 0.057\ \log v\left(Vs^{-1}\right) + 0.44 \tag{3}$$

For a totally irreversible electrode process, E_p and v are defined by the following Eq. (4):

$$E_p = E^{\circ\prime} + (RT/\alpha nF) - (RT/\alpha nF)\ \ln v \tag{4}$$

where $E^{\circ\prime}$ is formal potential, α is the cathodic electron transfer coefficient, n is the number of electrons. R, T and F have their usual meanings. α is generally assumed as 0.5 in the totally irreversible electrode process. From the slope of E_p versus natural logarithm of the scan rate (ln$v$) plot, the transfer coefficient (αn) was calculated as 1.04. [31]. Therefore, the oxidation of UA was found as two-electron transfer process.

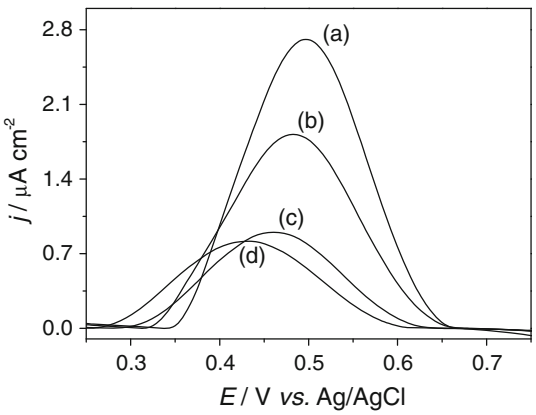

Fig. 4 DP voltammograms of 80 mM UA in 25 mM PBS at pH **a** 5.5, **b** 6.0, **c** 7.0 and **d** 8.0 at poly(AO)$_1$-modified GC electrode

3.3.3 Determination of UA with CV and DPV

Quantitative determination of UA was carried out at poly(AO)$_1$ film-modified GC electrodes using CV and DPV. All experiments were achieved in 25 mM PBS at pH 5.5, since the best response in relation to the peak current sensitivity and reproducibility was obtained in this buffer. The data obtained from the calibration graphs of CV and DPV are given in Table 3. The anodic peak current increased linearly with the concentration of UA in the range 1–75 μM for CV and 0.4–75 μM for DPV. Limit of detection (LOD) and limit of quantification (LOQ) values were calculated according to the 3 and 10 s/m criteria, respectively, where s is the standard deviation of the peak currents (five measurements) and m is the slope of the related calibration graph [32]. The LOD values were calculated as 3.7 × 10^{-1} for CV and 9.7 × 10^{-2} μM for DPV (Table 3). The precision of the methods was calculated from five replicate experiments in different solutions containing the same concentration of UA within the same day at poly(AO)$_1$-modified GC electrode and shown as RSD % in Table 3.

3.3.4 Determination of UA with fixed-potential amperometry

The quantitative determination of UA was also performed using fixed-potential amperometry at poly(AO)$_1$ film-modified GC electrodes. The amperometric response was obtained using the standard addition method under constant

Table 3 Data of the calibration lines for the quantitative determination of UA in 25 mM PBS at pH 5.5 by CV, DPV and fixed-potential amperometry for poly(AO)$_1$-modified GC electrode

	Methods		
	CV	DPV	Amperometry
Applied potential (V)	–	–	0.6
Peak potential (V)	0.57	0.45	–
Linearity range (μM)	1–75	0.4–75	0.04–5.3
Slope (μA mM^{-1})	6.82 ± 0.13	3.51 ± 6.0 × 10^{-2}	30.8 ± 0.45
Intercept (μA)	−7.8 × 10^{-4} ± 4.3 × 10^{-3}	4.7 × 10^{-3} ± 1.7 × 10^{-3}	1.6 × 10^{-3} ± 2.3 × 10^{-4}
Correlation coefficient	0.997	0.997	0.996
LOD (μM)	3.7 × 10^{-1}	9.7 × 10^{-2}	9.5 × 10^{-3}
LOQ (μM)	1.25	0.32	3.2 × 10^{-2}
Repeatability of peak potential (RSD %)[a]	0.23	0.22	–
Repeatability of peak current (RSD %)[a]	0.57	0.78	–

[a] UA concentration: 40 μM; Number of experiments: 5

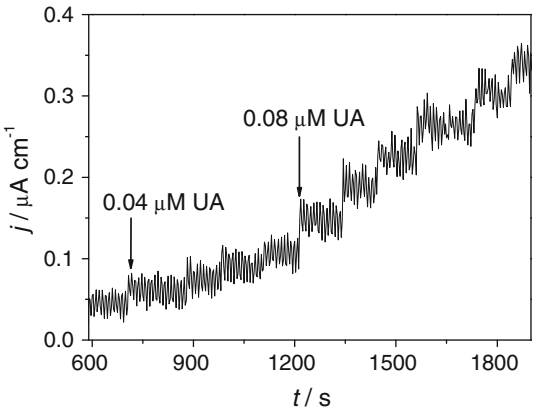

Fig. 5 Current density-time response curve by addition of UA in 25 mM PBS at pH 5.5 by fixed-potential amperometry at 0.6 V

solution stirring in 25 mM PBS at pH 5.5 at the potential of 0.6 V. Figure 5 shows the current density-time response curve. It can be seen from Fig. 5 that stable signals were obtained within 5 s after the step-by-step addition of UA. A linear response was obtained between the concentration of UA and the oxidation current after background subtraction. The results obtained from fixed-potential amperometry indicated a higher sensitivity with a lower detection limit than CV and DPV (Table 3).

Various analytical results of the oxidation of UA using different sensors can be found in the literature. The values of linear range and LOD obtained using DPV and fixed-potential amperometry are compared in Table 4. According to the results of DPV, a wider linear range and lower detection limit were obtained with poly(AO)$_1$-modified GC electrode compared to the electrodes reported in [33–37]. Although the modified electrodes described in [38, 39] gave a lower detection limit, they had narrow linear ranges compared to poly(AO)$_1$-modified electrode. For the results of fixed-potential amperometry, the modified electrode in this work exhibited a wider linear range than the electrodes reported in [39, 40], whereas it presented a narrow linear range compared to the electrodes described in [41, 42]. Furthermore, poly(AO)$_1$-modified GC electrode gave a lower detection limit than the modified electrodes described in [40, 41], whereas it presented a higher detection limit than the modified electrode in [42]. According to all analytical parameters in Table 4, poly(AO)$_1$ modified GC electrode exhibited good results. In addition, the modified electrode in this work is easy to prepare with good stability and can be used as an electrochemical UA sensor.

3.4 Interference study

The selectivity of UA was investigated using DPV with the modified electrode in the presence of ascorbic acid (AA) and dopamine (DA), since they commonly coexist in biological fluids, mainly in serum, blood and urine. The major problem is the overlapped oxidation peaks of UA, AA and DA, resulting poor selectivity [43, 44]. For this purpose, interference study was carried out in 25 mM PBS at pH 5.5 with poly(AO)$_1$-modified GC electrode, since the highest sensitivity had been obtained with this modified electrode. The concentrations of AA and DA were kept as 30 μM in the solution and the concentration of UA was increased in the concentration range between 10 and 80 μM (Fig. 6). The peak potentials of AA, DA and UA were ~80, 240 and 395 mV, respectively. The peak current of UA increased with increasing of its concentration, whereas the peak currents of AA and DA were almost stable. The plot of the peak current density versus the concentration of UA was linear in the selected concentration range of UA in the

Table 4 Compared parameters obtained using different electrochemical sensors for the determination of UA

Electrode	Method	Medium	Linear range (μM)	LOD (μM)	Ref.
5-HTP/GCE[a]	DPV	0.1 M PBS, pH 7.0	0.5–11	0.28	[33]
BCP/GCE[b]	DPV	0.067 M PBS, pH 4.5	0.5–12	0.20	[34]
MWCNT-PEDOT/GCE[c]	DPV	0.05 M PBS, pH 7.0	10–250	10.00	[35]
Pd/CNF-CPE[d]	DPV	0.1 M PBS, pH 4.5	2.0–200	0.70	[36]
SZP/MB[e]	DPV	Tris–HCl, pH 7.4	70–280	3.60	[37]
Poly(L-Arg)/ERGO/GCE[f]	DPV	0.1 M PBS, pH 6.5	0.1–10	0.05	[38]
PDDA-G/CPE[g]	DPV	0.1 M PBS, pH 7.0	0.5–20	0.08	[39]
	Amperometry, 0.4 V	0.1 M PBS, pH 7.0	0.5–46	–	[39]
OMC/Fc[h]	Amperometry, 0.38 V	0.1 M $LiClO_4$ + 0.1 M PBS, pH 7.3	60–390	1.80	[40]
GE/CFE[i]	Amperometry, 0.4 V	0.1 M PBS, pH 7.0	0.2–49.6	0.13	[41]
p-AMT/GCE[j]	Amperometry, 0.6 V	0.2 M PBS, pH 5.0	0.2–800	5.7×10^{-4}	[42]
poly $(AO)_1$/GCE	DPV	25 mM PBS, pH 5.5	0.4–75	9.7×10^{-2}	This work
poly $(AO)_1$/GCE	Amperometry, 0.6 V	25 mM PBS, pH 5.5	0.04–5.3	9.5×10^{-3}	This work

[a] 5-Hydroxytryptophan-modified glassy carbon electrode

[b] Poly(bromocresol purple)-modified glassy carbon electrode

[c] Multiwalled carbon nanotube and poly(3,4-ethylenedioxythiophene)-modified glassy carbon electrode

[d] Palladium nanoparticle-loaded carbon nanofibres-modified electrode

[e] Methylene blue adsorbed phosphorylated zirconia–silica composite electrode

[f] Poly(L-arginine)/graphene composite film-modified glassy carbon electrode

[g] Poly(diallyldimethylammonium chloride)-functionalised graphene/graphite composite electrode

[h] Ordered mesoporous carbon functionalized with ferrocenecarboxylic acid-modified electrode

[i] Graphene-modified carbon fibre electrode

[j] 5-Amino-2-mercapto-1,3,4-thiadiazole ultrathin film-modified glassy carbon electrode

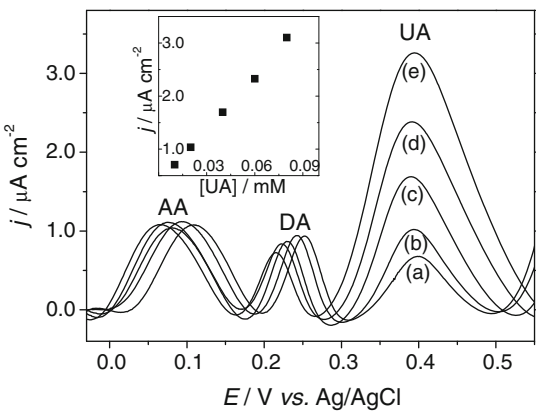

Fig. 6 DP voltammograms of **a** 10 μM, **b** 20 μM, **c** 40 μM, **d** 60 μM and **e** 80 μM UA in the presence of 30 μM AA and 30 μM DA in 25 mM PBS at pH 5.5. *Inset* magnifies the plot of peak current density versus the concentration of UA

presence of AA and DA. The linear regression equation of UA was expressed as: J (μA cm^{-2}) = 33.853 C_{UA} (mM) + 0.35 with a correlation coefficient of 0.998 (the inset in Fig. 6). The results showed that no interference was observed between UA, AA and DA in the same solution. Thus, the developed method is suitable for the determination of UA in the presence of AA and DA using poly(AO)-modified GC electrodes.

4 Conclusion

Electropolymerisation of AO was achieved on the surface of GC electrodes by potential cycling in 25 mM PBS at pH 5.5, 6.0, 7.0 and 8.0. The best polymerisation was obtained in 25 mM PBS at pH 5.5 containing 0.5 mM AO monomer. The electrochemical properties of poly(AO) film were investigated by CV, and it was found that the process of the polymer film was adsorption-controlled for both anodic and cathodic ways. For poly(AO) film, the best peak shape and the highest peak currents were obtained in 25 mM PBS at pH 5.5. Quantitative determination of UA was achieved with poly(AO)-modified GC electrode by CV, DPV and fixed-potential amperometry in 25 mM PBS at pH 5.5. The results obtained in this work were compared with the results of the modified electrodes in the literature. Interference study of UA, AA and DA was carried out with poly(AO) modified GC electrode and no interference occurred.

These results shows that poly(AO) film can be used in electrochemical sensors for UA, to be addressed in the future works for the other components.

References

1. Boguslavsky L, Kalash H, Xu Z, Beckles D, Geng L, Skotheim T et al (1995) Thin film bienzyme amperometric biosensors based on polymeric redox mediators with electrostatic bipolar protecting layer. Anal Chim Acta 311:15–21
2. Raj CR, Chakraborty S (2006) Carbon nanotubes-polymer redox mediator hybrid thin film for electrocatalytic sensing. Biosens Bioelectron 22:700–706
3. Liu X, Luo L, Ding Y, Kang Z, Ye D (2012) Simultaneous determination of L-cysteine and L-tyrosine using Au-nanoparticles/poly-eriochrome black T film modified glassy carbon electrode. Bioelectrochemistry 86:38–45
4. Reddaiaha K, Reddyb MM, Raghua P, Reddya TM (2013) An electrochemical sensor based on poly(solochrome dark blue) film coated electrode for the determination of dopamine and simultaneous separation in the presence of uric acid and ascorbic acid: a voltammetric method. Colloids Surf B Biointerfaces 106:145–150
5. Chitravathi S, Kumara Swamya BE, Mamatha GP, Sherigara BS (2012) Electrochemical behavior of poly(naphthol green B)-film modified carbon paste electrode and its application for the determination of dopamine and uric acid. J Electroanal Chem 667:66–75
6. Guo S, Zhu Q, Yang B, Wang J et al (2011) Determination of caffeine content in tea based on poly(safranine T) electroactive film modified electrode. Food Chem 129:1311–1314
7. Wang Y, Hu S (2006) A novel nitric oxide biosensor based on electropolymerization poly(toluidine blue) film electrode and its application to nitric oxide released in liver homogenate. Biosens Bioelectron 22:10–17
8. Lin KC, Yin CY, Chen SM (2011) An electrochemical biosensor for determination of hydrogen peroxide using nanocomposite of poly(methylene blue) and FAD hybrid film. Sens Actuators B Chem 157:202–210
9. Gherghi IC, Girousi ST, Voulgaropoulos AN, Tsitouridou RT (2003) Study of interactions between DNA-ethidium bromide (EB) and DNA-acridine orange (AO), in solution, using hanging mercury drop electrode (HMDE). Talanta 61:103–112
10. Palmgren MG (1991) Acridine orange as a probe for measuring pH gradients across membranes: mechanism and limitations. Anal Biochem 192:316–321
11. Lai S, Chang X, Tian L, Wang S, Bai Y, Zhai Y (2007) Fluorometric determination of DNA using nano-SiO_2 particles as an effective dispersant and stabilizer for acridine orange. Microchim Acta 156:225–230
12. Lyles MB, Cameron IL (2002) Interactions of the DNA intercalator acridine orange, with itself, with caffeine, and with double stranded DNA. Biophys Chem 96:53–76
13. Suna W, Wangb Y, Gongb S, Chengb Y, Shia F, Sunaa Z (2009) Application of poly(acridine orange) and graphene modified carbon/ionic liquid paste electrode for the sensitive electrochemical detection of rutin. J Electroanal Chem 629:35–42
14. Zhang Y (2004) Voltammetric behavior of dobutamine at poly(acridine orange) film modified electrode and its determination by adsorptive stripping voltammetry. Anal Lett 37:2031–2042
15. Wang Z, Xia J, Zhu L, Zhang F, Guo X, Li Y, Xia Y (2012) The fabrication of poly(acridine orange)/graphene modified electrode with electrolysis micelle disruption method for selective determination of uric acid. Sens Actuators B Chem 161:131–136
16. Kutzing MK, Firestein BL (2008) Altered uric acid levels and disease states. J Pharmacol Exp Ther 324:1–7
17. Dai X, Fang X, Zhang C, Xu R, Xu B (2007) Determination of serum uric acid using high-performance liquid chromatography (HPLC)/isotope dilution mass spectrometry (ID-MS) as a candidate reference method. J Chromatogr B 857:287–295
18. Yao D, Vlessidis AG, Evmiridis NP (2003) Microdialysis sampling and monitoring of uric acid in vivo by a chemiluminescence reaction and an enzyme on immobilized chitosan support membrane. Anal Chim Acta 478:23–30
19. Zhang Y, Wen G, Zhou Y, Shuang S, Dong C, Choi MMF (2007) Development and analytical application of an uric acid biosensor using an uricase-immobilized eggshell membrane. Biosens Bioelectron 22:1791–1797
20. Wu L, Feng L, Ren J, Qu X (2012) Electrochemical detection of dopamine using porphyrin-functionalized grapheme. Biosens Bioelectron 34:57–62
21. Özcan A, Sahin Y (2010) Preparation of selective and sensitive electrochemically treated pencil graphite electrodes for the determination of uric acid in urine and blood serum. Biosens Bioelectron 25:2497–2502
22. Ermer J, Miller JH (eds) (2005) Method validation in pharmaceutical analysis. Wiley-VCH, Weinheim
23. Bievre P, Günzler H (2005) Validation in chemical measurements. Springer, New York
24. Zhang Y, Zhuang H (2009) Poly(acridine orange) film modified electrode for the determination 1-naphthol in the presence of 2-naphthol. Electrochim Acta 54:7364–7369
25. Kul D, Pauliukaite R, Brett CMA (2011) Electrosynthesis and characterisation of poly(Nile blue) films. J Electroanal Chem 662:328–333
26. Zhou DM, Chen HY (1997) The electrochemical polymerization of redox dye-nile blue for the amperometric determination of haemoglobin. Electroanalysis 9:399–402
27. Pauliukaite R, Selskiene A, Malinauskas A, Brett CMA (2009) Electrosynthesis and characterisation of poly(safranine t) electroactive polymer films. Thin Solid Films 517:5435–5441
28. Barsan MM, Pinto EM, Brett CMA (2008) Electrosynthesis and electrochemical characterisation of phenazine polymers for application in biosensors. Electrochim Acta 53:3973–3982
29. Giménez-Romero D, García-Jareño JJ, Vicente F (2004) Calculation of the surface concentration of Zn(I) from the anodic voltammetric peak of zinc combined with the QCM results. Electrochem Commun 6:903–907
30. Ghica ME, Brett CMA (2009) Asymmetric electrochemical carboxylation of prochiral acetophenone: an efficient route to optically active atrolactic acid via selective fixation of carbon dioxide. J Electroanal Chem 629:35–41
31. Liu Y, Xu L (2007) Electrochemical sensor for tryptophan determination based on copper-cobalt hexacyanoferrate film modified graphite electrode. Sensors 7:2446–2457
32. Ozkan SA (ed) (2012) Electroanalytical methods in pharmaceutical analysis and their validation. HNB Publishing, New York
33. Lin XQ, Li YX (2006) Monolayer covalent modification of 5-hydroxytryptophan on glassy carbon electrodes for simultaneous determination of uric acid and ascorbic acid. Electrochim Acta 51:5794–5801
34. Wang Y, Tong LL (2010) Electrochemical sensor for simultaneous determination of uric acid, xanthine and hypoxanthine based on poly(bromocresol purple) modified glassy carbon electrode. Sens Actuators B Chem 150:43–49
35. Lin KC, Tsai TH, Chen SM (2010) Performing enzyme-free H_2O_2 biosensor and simultaneous determination for AA, DA, and UA by MWCNT–PEDOT film. Biosens Bioelectron 26:608–614
36. Huang J, Liu Y, Hou H, You T (2008) Simultaneous electrochemical determination of dopamine, uric acid, and ascorbic acid

using palladium nanoparticle-loaded carbon nanofibers modified electrode. Biosens Bioelectron 24:632–637
37. Argüello J, Leidens VL, Magosso HA, Ramos RR, Gushikem Y (2008) Simultaneous determination of ascorbic acid, dopamine and uric acid by methylene blue adsorbed on a phasphorylated zirconia-silica composite electrode. Electrochim Acta 54:560–565
38. Zhang FY, Wang ZH, Zhang YZ, Zheng ZX, Wang CM, Du YL, Ye WC (2012) Simultaneous electrochemical determination of uric acid, xanthine and hypoxanthine based on poly(L-arginine)/graphene composite film modified electrode. Talanta 93:320–325
39. Yu Y, Chen Z, Zhang B, Li X, Pan J (2013) Selective and sensitive determination of uric acid in the presence of ascorbic acid and dopamine by PDDA functionalized graphene/graphite composite electrode. Talanta 112:31–36
40. Ndamanisha JC, Guo L (2008) Electrochemical determination of uric acid at ordered mesoporous carbon functionalized with ferrocenecarboxylic acid-modified electrode. Biosens Bioelectron 23:1680–1685
41. Du J, Yue R, Yao Z, Jiang F, Du Y, Yang P, Wang C (2013) Nonenzymatic uric acid electrochemical sensor based on graphene-modified carbon fiber electrode. Colloids Surf A Physicochem Eng Asp 419:94–99
42. Kalimuthu P, Abraham John S (2009) Electropolymerized film of functionalized thiadiazole on glassy carbon electrode for the simultaneous determination of ascorbic acid, dopamine, and uric acid. Bioelectrochemistry 77:13–18
43. Ensafi AA, Taei M, Khayamian T (2010) Simultaneous determination of ascorbic acid, dopamine, and uric acid by differential pulse voltammetry using tiron modified glassy carbon electrode. Int J Electrochem Sci 5:116–130
44. Ping J, Wu J, Wang Y, Ying Y (2012) Simultaneous determination of ascorbic acid, dopamine and uric acid using high-performance screen-printed grapheme electrode. Biosens Bioelectron 34:70–76